Surface optical constants of silicon and germanium derived from electron-energy-loss spectroscopy

H. Froitzheim and H. Ibach
Institut für Grenzflächenforschung und Vakuumphysik der Kernforschungsanlage Jülich GmbH, 517 Jülich, Germany

D. L. Mills*
Department of Physics, University of California, Irvine, California 92664
(Received 26 November 1974)

High-resolution electron-energy-loss spectra are reported for cleaved surfaces of silicon and germanium. The inelastic scattering has been observed with a small calibrated angular aperture spectrometer under various angles of incidence. Therefore absolute inelastic cross sections could be derived. For higher loss energies (>3.5 eV), where bulk transitions prevail, the cross sections are in agreement with a recent theory of Mills that relates the cross sections to a loss function $\mathrm{Im}[-1/(\epsilon+1)]$ calculated from the bulk dielectric function $\epsilon(\omega)$. For smaller energies additional surface-state transitions are observed. These cross sections are described by assuming an optically active surface layer. The optical absorption of this layer is calculated from the loss spectra in an energy range up to 3 eV through use of an extension of the earlier theory. The result compares reasonably well to previously reported optical data.

I. INTRODUCTION

Silicon and germanium are among the few examples of materials where the existence of intrinsic surface states with a density corresponding to the number of surface atoms is now well documented. For both materials surface states above and below the Fermi level have been detected. However, most of the available information is concerned with the occupied part of the surface-state bands. These states have been investigated by ultraviolet photoemission spectroscopy (UPS).[1–4] The surface character of the states has been established by adsorption experiments[1,2] or by comparing the spectra of crystallographically distinct surfaces.[3,4] The surface states identified by UPS extend over the energy region of the entire valence band. The origin of the states has been clarified in recent theoretical investigations.[5–7] By combining a pseudopotential calculation in the bulk with a self-consistent numerical integration of Schrödinger's equation in the surface region, Appelbaum and Hamann[7] plotted charge densities of electrons in surface states in the various energy regions. It appears from these plots that the surface states near the top of the valence band are the dangling bonds while the lower-energy surface states are associated with the back bonds of the surface atoms. The results of Appelbaum and Hamann were reproduced by an atomic-orbital calculation of Pandey and Phillips.[6] In addition they display the surface band structure $E(k)$. The calculations will possibly be extended to include the reconstructed surface lattices of clean Si and Ge. With this remarkable theoretical progress further detailed experimental parameters of the surface band structure such as optical constants of the surface layer become of interest.

For cleaved Si and Ge surfaces the optical properties of the surface layer have already been investigated by multiple-internal-reflection spectroscopy and by ellipsometry in a limited energy range.[8,9] The difference between clean and oxygen-covered surfaces was attributed as being due to transitions from occupied to empty surface states. More recently it has been shown experimentally[10] and in a theoretical treatment of Mills[11] that optical properties of surfaces may also be investigated by electron-energy-loss spectroscopy (ELS). Indeed surface-associated transitions have been observed in ELS.[12,13] In order to derive optical constants from ELS one has to determine absolute cross sections for the inelastic scattering. Under certain conditions one may then derive $d\epsilon_2^s(\omega)$, where $\epsilon_2^s(\omega)$ is the imaginary part of the dielectric function of the material in the surface region and d is the thickness of the surface-state layer. The quantity $d\epsilon_2^s(\omega)$ may be related directly to other optical parameters measured by techniques such as surface absorption and ellipsometry.

In this paper we report high-resolution electron-energy-loss spectra of Si and Ge and an analysis of these data in terms of optical constants. The paper is organized as follows: In Sec. II the apparatus and examples of the raw data are presented. In Sec. III we shall review briefly the scattering theory of Mills and describe an extension of the theory to the case where a surface layer with dielectric constant different from that of the bulk is present. We pay particular attention to the limits of applicability of this approach. The method by which the required conditions are met experimentally and the procedure of data reduction are described in Sec. IV. In this section, we also derive

from the data values of the quantity $d\epsilon_2^s(\omega)$, where d is the thickness of the layer within which the oscillator strength of the surface-state transitions is confined, and $\epsilon_2^s(\omega)$ is the imaginary part of the dielectric constant of this region. In Sec. V the results are compared to optical experiments and the current state of the theory.

II. EXPERIMENTS AND RESULTS

High-resolution electron-energy-loss spectra have been recorded by a two-axis electron spectrometer (Fig. 1). Electrons are monochromatized and analyzed by means of electrostatic 127° deflectors, which are modified to meet fringe field[14] corrections and second-order image aberrations.[15] The electron energy at the crystal can be varied between 5 and 100 eV independent of the pass energies in the 127° deflectors. A second stage of smaller radius is added to the analyzer to suppress ghost peaks in the loss spectrum caused by a mirror reflection of the elastic beam at the outer deflecting plate in the first analyzer. The limiting overall resolution of this system is 5–10 meV (depending on the pretreatment of the spectrometer), with a current of 10^{-12} A at the detector when the beam was directly transmitted into the analyzer without being reflected from a crystal. Because of the low backscattering coefficient at electron energies of 50 eV higher currents were used in the experiments reported here at the expense of resolution. Typically the full width at half-maximum (FWHM) was $\Delta E_{1/2} = 80$ meV.

Clean (111) crystal surfaces were prepared by cleaving in ultrahigh vacuum of 10^{-10} Torr. The spectra were always recorded in the direction of maximum reflection.

Typical results at high angles of incidence are shown in Figs. 2 and 3. A qualitative interpretation has been given previously,[13,16] and we therefore only summarize the presently accepted interpretation. The transitions labeled S_0 and S_1 both involve surface states. On the cleaved surface exhibiting a 2×1 superlattice the dangling bond is split into two subbands separated by a gap of 0.25 and 0.4 eV for Si and Ge, respectively.[8,13] S_0 has been attributed to transitions near the zone boundary between these two subbands.[6,28] On both materials S_0 disappears when the surface structure is converted by annealing. The transitions labeled E_1 and E_2 are transitions between bulk bands near the surface in the selvedge of the crystal.

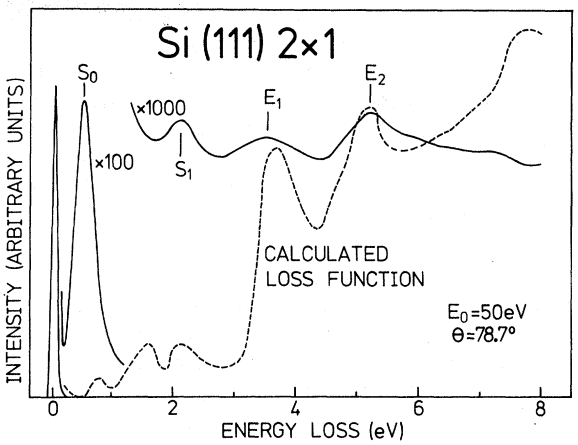

FIG. 2. Typical energy-loss spectrum of a cleaved (111) 2×1 silicon surface at an angle of incidence $\theta = 78.7°$. S_0 and S_1 are surface-state transitions. The dashed line is a calculated spectrum from bulk optical data[28] after Eq. (3.5) (see also Sec. IV).

III. THEORY OF ELECTRON-LOSS SPECTROSCOPY

It has been recognized for a long time that electrons are inelastically scattered by long-wavelength charge-density fluctuations in solids.[17] Electron

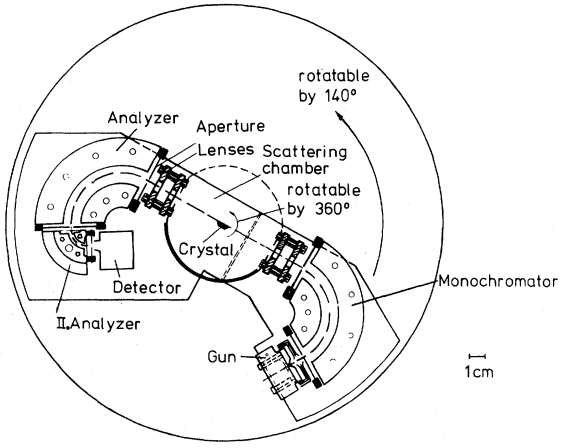

FIG. 1. Electron spectrometer for a quantitative determination of inelastic cross sections.

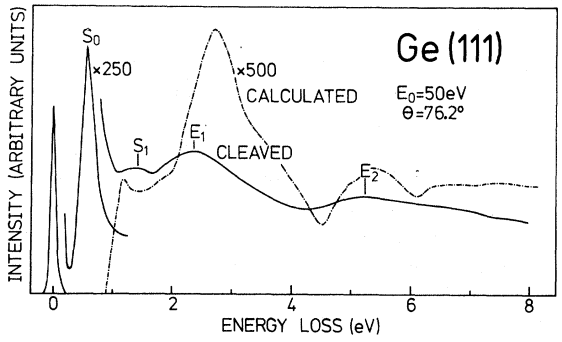

FIG. 3. Typical energy-loss spectrum for a cleaved (111) 2×1 germanium surface. The dot–dashed line is the calculated spectrum from bulk optical data (Ref. 26) after Eq. (3.5) (see also Sec. IV).

spectroscopy therefore provides information about the complex dielectric constant $\epsilon(q,\omega)$ of the solid. Most of the experimental and theoretical work has been concerned with transmission of medium-high-energy electrons through thin films. It has been shown, however, that basically similar loss spectra can be observed after reflection from the surface of a solid.

The first theoretical treatment of this scattering geometry was that by Lucas and Sunjic.[18,19] The theory of Lucas and Sunjic employs a classical description of the electron motion, and is confined to the description of the scattering by surface optical phonons on ionic crystals (surface polaritons), or surface plasmons in the free-electron gas. Since the Lucas-Sunjic theory employs a classical description of the electron motion, it does not treat properly that part of the electron-surface interaction which gives rise to the elastic scattering (i.e., the specular beam). Evans and Mills[20,21] have presented a description of the scattering process in the reflection geometry which is fully quantum mechanical in its treatment of the electron motion and does give a proper account of this electron-surface interaction. However, the treatment of Evans-Mills may be applied only to the case where the scattering is produced by well-defined excitations of boson character, i.e., surface phonons or surface plasmons in the free-electron metal.

A more general treatment of the scattering by electric field fluctuations outside the surface of the crystal has now been presented by Mills.[11] According to this theory, the inelastic cross section for small-angle scattering from a semi-infinite material may be written in the form

$$\frac{d^2S}{d\Omega\, d\omega} = \frac{m^2e^2v_\perp^2}{2\pi\cos\theta}\,\frac{k_s}{k_I} \times \frac{|v_\perp q_\parallel (R_s+R_I) + i(R_I-R_s)(\omega-\vec{v}_\parallel\cdot\vec{q}_\parallel)|^2}{q_\parallel^2[v_\perp^2q_\parallel^2+(\omega-\vec{v}_\parallel\cdot\vec{q}_\parallel)^2]^2} \times P(\vec{q}_\parallel,\omega)\,, \tag{3.1}$$

where $P(q,\omega)$ is a surface analog of the structure factor $S(q,\omega)$ that appears in the theory of neutron scattering from the bulk of crystals.[22] In the derivation of Eq. (3.1) only single inelastic scattering has been considered. Double inelastic scattering is, however, small.[11,20,21] In Eq. (3.1), R_s and R_I are the complex elastic reflection coefficients (the amplitude of the reflected electron wave) for the diffraction-loss and loss-diffraction processes, respectively, $v_\parallel$ and $v_\perp$ denote the parallel and perpendicular components of the initial electron velocity, and k_I and k_s are the electron wave vectors before and after the inelastic process. The angle θ is the angle of incidence measured from the normal. Equation (3.1) is given in atomic units ($\hbar = 1$).

The function $P(\vec{q}_\parallel,\omega)$ is related to the correlation function $\langle\rho(\vec{x}',t)\rho(\vec{x},0)\rangle$ for charge-density fluctuations in the crystal in the following manner[11]:

$$P(\vec{q}_\parallel,\omega) = \int d^2r_\parallel \int_{-\infty}^{0+} dz \int_{-\infty}^{0+} dz'\, e^{i\vec{q}_\parallel\cdot\vec{r}_\parallel'} \times e^{-i\omega t}e^{q_\parallel(z+z')}\langle\rho(\vec{r}_\parallel',z',t)\rho(0z,0)\rangle\,. \tag{3.2}$$

where the crystal occupies the region $z<0$, and $\vec{r}_\parallel$ is the component of $\vec{r}$ projected on a plane parallel to the surface.

For scattering from field fluctuations outside a semi-infinite dielectric with complex frequency-dependent dielectric constant $\epsilon(\omega)$, one may show that[11] for energy-loss processes with $\hbar\omega \gg k_BT$

$$P(q_\parallel,\omega) = (2/\pi)\,\mathrm{Im}\{-1[1+\epsilon(\omega)]\}\,. \tag{3.3}$$

As one can see from Eq. (3.1), the loss spectrum in general is determined by the energy dependence of the reflection coefficients R_s and R_I as well as by the dielectric properties. The question of which of the two contributions is most significant can be tested experimentally by observing loss spectra at different primary energies. This has been done by several authors,[10,12,13,23] and it seems that for the semiconductors Si, Ge, GaAs, and ZnO the loss spectra do not vary significantly with primary energy. Therefore, for loss energies of a few eV, the energy dependence of R is sufficiently small that

$$|(R_I-R_s)/(R_I+R_s)| \ll 1\,. \tag{3.4}$$

Introducing this assumption into Eq. (3.1) and employing the form of $P(q_\parallel,\omega)$ appropriate to the semi-infinite dielectric gives

$$\frac{1}{|R|^2}\,\frac{d^2S}{d\Omega\, d\omega} = \frac{m^2e^2v_\perp^2}{\pi^2\cos\theta}\,\frac{k_s}{k_I} \times \frac{4v_\perp^2q_\parallel}{[v_\perp^2q_\parallel^2+(\omega-\vec{v}_\parallel\cdot\vec{q}_\parallel)^2]^2}\,\mathrm{Im}\left(\frac{-1}{1+\epsilon(\omega)}\right). \tag{3.5}$$

In the derivation of Eq. (3.1), penetration of the electrons into the solid has been neglected completely. The excitation of "bulk" losses by the electron described by the bulk loss function $\mathrm{Im}\,[-1/\epsilon(\omega)]$ is therefore not included. It is known, however, that for most scattering geometries "bulk" and "surface" losses, (e.g., bulk and surface plasmon excitations) of approximately equal strength are observed. Disregarding the penetration of the electrons into the solid even if the attenuation length is only a few Å at incident energies $E_0 = 50$ eV is therefore not justified in general. However, as can be seen from Eqs. (3.1) and (3.3), the inelastic cross section for "surface" losses diverges for grazing incidence. One there-

fore might expect the losses proportional to $\mathrm{Im}\{-1/[1+\epsilon(\omega)]\}$ to be dominant at large angles of incidence. This is indeed confirmed by measurements by Powell on liquid aluminum.[25] Thus we expect the results quoted above to be applicable to the analysis of the data at high angles of incidence (see Sec. IV.)

A further assumption in the derivation of the above results is that the scattering angle associated with the loss event is small. This requires $q_\parallel$ to be small compared to a reciprocal lattice vector. The momentum transfer involved in the inelastic scattering is determined by the kinematics of the scattering process. For a planar scattering geometry, from energy and momentum conservation it follows that

$$q_\parallel = (1/a_B)(1/\sqrt{R})\{[\sqrt{(E_0)} - \sqrt{(E_0 - \hbar\omega)}]\sin\theta + \sqrt{(E_0)}\vartheta\cos\theta\}, \tag{3.6}$$

where ϑ is the difference between the actual scattering angle and the angle of specular reflection in the plane of incidence (see Fig. 4). For a typical loss of interest, $\hbar\omega = 1$ eV and $E_0 = 50$ eV, $q_\parallel$ is of the order of 0.035 Å^{-1}, which seems sufficiently small for the small-angle approximation in the scattering kinematics required in the derivation of Eq. (3.1) to be valid, and for the wave-vector dependence of $\epsilon(\omega, q)$ to be ignored.

The form given for $P(q_\parallel, \omega)$ in Eq. (3.3) and utilized to obtain Eq. (3.5) presumes the dielectric constant of the material to be uniform right up to the surface. However, as one can see from Figs. 2 and 3, surface losses are observed in the data. These losses correspond to transitions between surface-state bands in a layer roughly 1 Å thick.[5,6]

We have extended the calculation of the inelastic scattering cross section to include a thin surface layer of thickness d and complex dielectric constant $\epsilon^s(\omega)$ superimposed on the surface of a semi-infinite dielectric with bulk dielectric constant $\epsilon^b(\omega)$.

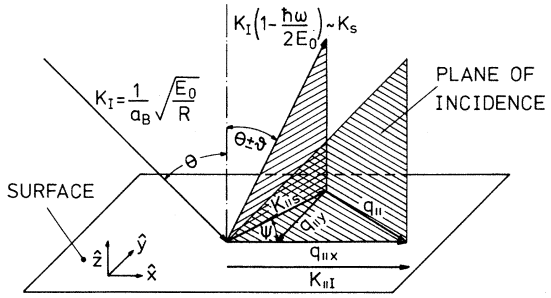

$$q_{\parallel x}\sim\frac{1}{a_B}\sqrt{\frac{E_0}{R}}\left[\frac{\hbar\omega}{2E_0}(\sin\theta+\vartheta\cos\theta)-\vartheta\cos\theta\right]$$

$$q_{\parallel y}\sim\frac{1}{a_B}\sqrt{\frac{E_0}{R}}\left(1-\frac{\hbar\omega}{2E_0}\right)\psi\sin\theta$$

FIG. 4. The kinematics of the inelastic scattering.

The calculation of the form of $P(q_\parallel, \omega)$ proceeds in the manner described earlier. In the course of the calculation, certain Green's functions associated with the electromagnetic field are required. These Green's functions are defined in Eq. (3.26) of Ref. 11. The Green's functions have been constructed recently for the semi-infinite dielectric with a uniform overlayer, and their construction will be described in a forthcoming publication.[25]

In the presence of a surface overlayer of thickness d which we use here to incorporate the surface-state transitions into our model, the differential cross section for inelastic scattering from the surface may still be described by Eq. (3.5), except the dielectric function $\epsilon(\omega)$ is now replaced by an effective complex dielectric constant $\tilde{\epsilon}(q_\parallel, \omega)$ given by

$$\tilde{\epsilon}(q_\parallel, \omega) = \epsilon^s(\omega)\,\frac{1-\Delta e^{-2q_\parallel d}}{1+\Delta e^{-2q_\parallel d}}\,, \tag{3.7}$$

where

$$\Delta = [\epsilon^s(\omega) - \epsilon^b(\omega)]/[\epsilon^s(\omega) + \epsilon^b(\omega)]\,. \tag{3.8}$$

Note that when $q_\parallel d \gg 1$, $\tilde{\epsilon}(q_\parallel, \omega) \approx \epsilon^s(\omega)$, while for $q_\parallel d \ll 1$, $\tilde{\epsilon}(q, \omega) \approx \epsilon^b(\omega)$.

In general, the surface dielectric function $\epsilon^s(\omega)$ cannot be derived from experimentally determined cross sections obtained from scattering into an aperture of finite size, since $\epsilon^s(\omega)$ appears entwined with $q_\parallel$, when the integral appropriate to the experimental angular range is performed. The results may be simplified, however, under certain conditions that apply to the cleaved surfaces of silicon and germanium. One may first consider the fact that in the energy range of interest and within angular apertures of the spectrometer of the order of 1^0, $2q_\parallel d$ is small compared to unity. In this limit, we have

$$\tilde{\epsilon}(q_\parallel, (\omega) \sim \epsilon^b(\omega)[1 - q_\parallel d\epsilon^b(\omega)/\epsilon^s(\omega)] + q_\parallel d\,\epsilon^s(\omega)\,. \tag{3.9}$$

In the energy range where surface losses dominate, we may further assume

$$\epsilon_2^b \ll \epsilon_2^s\,, \tag{3.9a}$$

$$q_\parallel d\,\epsilon_1^s \ll \epsilon_1^b\,. \tag{3.9b}$$

The loss function $\mathrm{Im}\{-1/[\tilde{\epsilon}(q_\parallel, \omega)+1]\}$ then simplifies to

$$\mathrm{Im}\left(\frac{1}{\tilde{\epsilon}(q_\parallel, \omega)+1}\right) \sim \frac{q_\parallel d[\epsilon_2^s - (\epsilon_1^b)^2\,\mathrm{Im}(\epsilon^s)^{-1}]}{(\epsilon_1+1)^2 + q_\parallel^2 d^2[\epsilon_2^s - (\epsilon_1^b)^2\mathrm{Im}(\epsilon^s)^{-1}]}\,. \tag{3.10}$$

Inserting some reasonable numbers for $d \sim 1$ Å and $\epsilon_2^s > 20$, one further observes that

$$(\epsilon_1^b)^2 \operatorname{Im}(\epsilon^s)^{-1} \ll \epsilon_2^s \tag{3.11}$$

and

$$q_{\parallel} d\, \epsilon_2^s \ll \epsilon_1^b . \tag{3.12}$$

One then arrives at the approximate form

$$\operatorname{Im}\{-1/\epsilon(q_{\parallel},\omega)+1\} \approx q_{\parallel} d\, \epsilon_2^s/(\epsilon_1^b+1)^2 . \tag{3.13}$$

For surface-state transitions, the cross section is therefore proportional to ϵ_2^s. One has the explicit form

$$\frac{1}{|R|^2}\frac{d^2S}{d\Omega\, d\omega} \approx \frac{me^2v_\perp^2}{\pi^2\cos\theta}\frac{k_s}{k_I} \times \frac{4v_\perp^2 q_{\parallel}^2}{[v_\perp^2 q_{\parallel}^2 + (\omega - \vec{v}_{\parallel}\cdot\vec{q}_{\parallel})^2]^2}\frac{d\epsilon_2^s(\omega)}{[\epsilon_1^b(\omega)+1]^2} . \tag{3.14}$$

IV. DATA REDUCTION

In order to perform a quantitative comparison of theory and experiment one has to take into account the finite size of the angular aperture of the spectrometer. Furthermore, when loss spectra are observed in the direction of specular reflection as we did, a considerable momentum transfer is involved at higher loss energies [see Eq. (3.6)]. One therefore has to introduce the kinematics of the scattering into Eqs. (3.5) and (3.14). Let ϑ and ψ be the angles between specular reflection and the actual scattering angle parallel and perpendicular to the plane of incidence (Fig. 4). Then the components of $q_{\parallel}$ may be expressed in terms of ϑ and ψ:

$$q_{\parallel x} \sim k_I[(\hbar\omega/2E_0)\sin\theta + \vartheta\cos\theta] , \tag{4.1}$$

$$q_{\parallel y} \sim k_s \psi \sin\theta . \tag{4.2}$$

We have neglected terms of higher than linear order in ϑ, ψ, and $\hbar\omega/2E_0$ and assume that $\tan\theta \gg \vartheta$. After inserting Eqs. (4.1) and (4.2) into Eq. (3.5) and integrating up to a finite aperture size $\Delta\vartheta\Delta\psi$, one obtains

$$\frac{1}{|R|^2}\frac{ds}{d\hbar\omega} = \frac{4}{\pi a_B k_I \cos\theta}\frac{1}{\hbar\omega}F(\hbar\omega,\theta,\Delta\vartheta,\Delta\psi) \times \operatorname{Im}\frac{-1}{\epsilon(\omega)+1} , \tag{4.3}$$

with

$$F(\hbar\omega,\theta,\Delta\vartheta,\Delta\psi) = \frac{1}{\pi}\frac{\hbar\omega}{2E_0}\left(1-\frac{\hbar\omega}{2E_0}\right)\int_{-\Delta\vartheta/2}^{+\Delta\vartheta/2}\int_{-\Delta\psi/2}^{+\Delta\psi/2}\frac{N^{1/2}}{(N+M)^2}\,d\vartheta\,d\psi , \tag{4.4}$$

$$N = [(\hbar\omega/2E_0)\sin\theta + \vartheta\cos\theta]^2 + (1-\hbar\omega/2E_0)^2\psi^2\sin^2\theta \tag{4.5}$$

$$M = [(\hbar\omega/2E_0)\cos\theta - \vartheta\sin\theta]^2 .$$

For surface transitions $F(\hbar\omega,\theta,\Delta\vartheta,\Delta\psi)$ has to be replaced by

$$F_s(\hbar\omega,\theta,\Delta\vartheta,\Delta\psi) = \frac{1}{\pi}\frac{\hbar\omega}{2E_0}\left(1-\frac{\hbar\omega}{2E_0}\right)k_I\int_{-\Delta\vartheta/2}^{\Delta\vartheta/2}\int_{-\Delta\psi/2}^{\Delta\psi/2}\frac{N}{(N+M)^2}\,d\vartheta\,d\psi \tag{4.6}$$

and $\operatorname{Im}\{-1/[\epsilon(\omega)+1]\}$ by Eq. (III-13). For small energy losses ($\hbar\omega \ll 2E_0$), $F(\hbar\omega,\theta,\Delta\vartheta,\Delta\psi)$ approaches $\frac{1}{2}\pi$ and becomes identical to the function $F(\alpha,\gamma)$ defined in the paper of Lucas and Sunjic.[19] For larger $\hbar\omega/2E_0\Delta$ the momentum transfer even for $\vartheta = 0$ [Eq. (3.6)] has to be taken into account and $F(\hbar\omega,\theta,\Delta\vartheta,\Delta\psi)$ is much smaller than $F(\alpha,\gamma)$. The physical reason for the much lower intensities predicted by the scattering formula of Mills as compared to the earlier work is that if $\hbar\omega \sim 2E_0\Delta\vartheta$ the higher momentum transfer in the scattering drives the surface wave out of the resonance with the passing electron [Eq. (3.5)]. The cross section defined in Eq. (4.3) is related to the observed intensities by

$$\frac{1}{|R|^2}\frac{dS}{d\hbar\omega} = \frac{I_{\text{inel}}(\omega)}{\int I_{\text{el}}d\hbar\omega} \equiv S_{\text{exp}} , \tag{4.7}$$

where $I_{\text{inel}}(\omega)$ denotes the count rate in the inelastic channel and $\int I_{\text{el}}d\hbar\omega$ is the integral over the elastic peak in the spectrum. Some values for this cross section are presented in Table I. Both functions F and F_s do not depend very much on θ (Table II). The validity of the basic assumptions may therefore be tested by plotting the cross section S_{exp} versus

TABLE I. Some cross sections for inelastic scattering from cleaved silicon and germanium surfaces. For silicon the effective angular aperture was $\Delta\vartheta = \Delta\psi = 2.7°$, for germanium $\Delta\vartheta = \Delta\psi = 2.1°$. The angles of incidence were $\theta = 78.7°$ and $\theta = 76.2°$, respectively.

$\hbar\omega$	S_{Si} (10^{-2} eV^{-1})	S_{Ge} (10^{-2} eV^{-1})
0.3	3.04	
0.4	6.45	0.83
0.5	9.66	2.53
0.6	9.24	2.54
0.7	6.45	1.57
0.8	3.79	1.01
0.9	2.32	0.81
1.0	1.55	0.72
1.2	1.11	0.67
1.4	0.96	0.70
1.6	0.89	0.67
1.8	0.88	0.68
2.0	0.94	0.74
2.2	0.95	0.78
2.4	0.88	0.80
2.6	0.84	0.78
2.8	0.84	0.74
3.0	0.85	0.69

TABLE II. Typical values for the finite-aperture-size correction $F(\hbar, \omega, \theta, \Delta\vartheta, \Delta\psi)$ for various $\alpha = \hbar\omega/E_0\Delta\vartheta = \hbar\omega/E_0\Delta\psi$. At any angle of incidence only a small fraction of the inelastic intensity is scattered in the forward direction. This is contrary to earlier (Ref. 18), where the kinematics of the scattering were neglected.

θ \ α	0.1	0.3	1.0	3.0	10
50	$\sim\pi/2$	1.406	0.553	0.101	0.0099
60	$\sim\pi/2$	1.318	0.584	0.113	0.0111
70	1.533	1.267	0.604	0.122	0.0120
80	1.475	1.243	0.614	0.127	0.0126

$(\cos\theta)^{-1}$ (Fig. 5). No systematic deviation from a straight line is observed even for small angles of incidence. This shows that neither a possible inelastic scattering of electrons inside the material [losses~ $\mathrm{Im}(-1/\epsilon)$] nor diffraction effects can be very important. The scattering of the points is assumed to be caused by the limited reproducibility of the focusing conditions of the spectrometer.

Indeed the assumption of a constant and rectangular aperture $\Delta\theta\Delta\psi$ is a simplification. Actually the spectrometer has a continuous transmission function $T(\theta, \psi)$. Only the θ dependence of $T(\theta, \psi)$ could be tested in the experiment. $T(\theta, 0)$ is roughly Gaussian shaped with a FWHM of 1.4°. Considering the geometry for the scattering in the spectrometer and the height of the slits, one may estimate $T(0, \psi)$ to be approximately rectangular shaped, having a width of ~1.6°. To compare the observed intensities with Eq. (4.3) we have integrated F and F_s numerically on a 50×50 mesh. Some typical values of F are tabulated in Table I. Good agreement between the observed cross sections and the cross sections calculated from bulk optical data[23] has been found for GaAs if $\Delta\theta = \Delta\psi = 1.4°$ was used (Fig. 6). On Ge and Si, however, the observed intensities were higher and differed from crystal to crystal. Cleaved surfaces of Ge and Si are not completely flat. They may contain steps up to a relative density of step atoms of 10%. We assume that the ratio of the total inelastic scattering to the elastic scattering is not altered on these surfaces. However, the elastic intensity is partially scattered out of the specular direction and is not accepted by the spectrometer any more. The observed inelastic scattering is only very little affected, because of the comparatively broad angular distribution even on flat surfaces. This introduces an apparent increase in the relative inelastic cross sections as though the effective aperture size of the spectrometer had been enlarged. We therefore treated the aperture size $A^2\Delta\theta\Delta\psi$ as a parameter (Fig. 6).

The fluctuations in the ratio of the observed and calculated cross sections may be in part due to the limited accuracy of the bulk optical constants. The main contribution, however, seems to arise from the fact that ELS integrates over transitions of a finite momentum transfer. On all three materials the observed loss spectrum is therefore smoother than the calculated (Fig. 2 and 3) one. In addition, surface-state transitions are observed on Ge and Si. The main surface contribution is in the energy range 0–3 eV. Assuming that Eq. (3.14) applies to these transitions, we may now calculate $d\epsilon_2^s$ in the energy range where bulk transitions may be neglected. For Ge this is possible only in a very limited energy range (Fig. 3) for Si, however, the range extends to ~3 eV. The result for Si is plotted in Fig. 7. For germanium a similar result can be derived for energies only up to 1 eV. Since also most theoretical calculations consider silicon only we concentrate on silicon in the following discussion, although obviously some conclusions apply to germanium as well.

V. DISCUSSION

Two previous attempts to derive optical constants of the surface layer have been reported. Chiarotti *et al.*[8] have determined the change in the reflectivity of cleaved silicon and germanium surfaces before and after oxygen coverage in a multiple-internal-reflection experiment. The surface- ab-

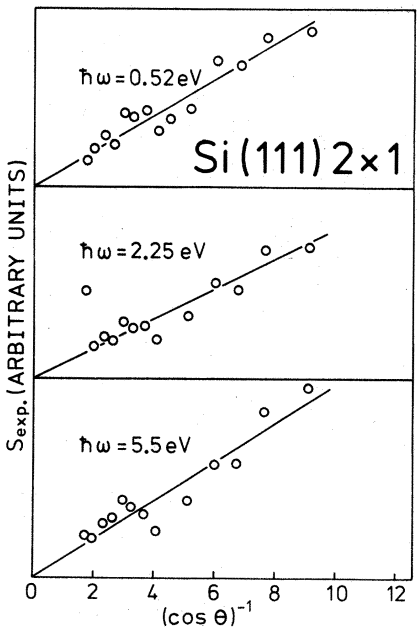

FIG. 5. Experimental cross sections versus $(\cos\theta)^{-1}$ for various energy losses.

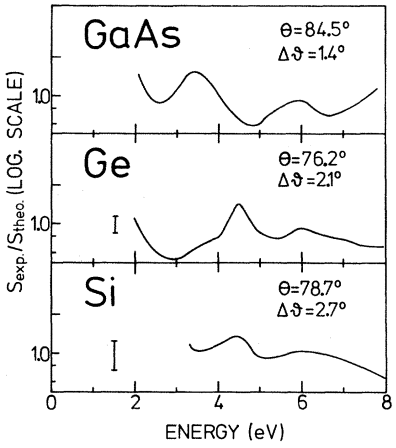

FIG. 6. Ratio of experimental and theoretical cross sections for losses of bulk origin. The theoretical cross sections are calculated according to Eq. (3.5), making use of bulk optical data (Ref. 26). Because of the finite momentum transfer in the scattering the structure in the ELS data is smoothed compared to the theoretical cross sections calculated from the optical data (compare also Figs. 2 and 3). This causes the fluctuations around unity. The experimental data for Si and Ge correspond to Figs. 1 and 2, respectively.

sorption constant $\alpha \sim \Delta R/R$ defined in their paper can be simply related to $\epsilon_2^s(\omega)$ of the surface layer by making use of a formula given by McIntyre and Aspnes.[27] For the small angle of incidence used in the reflection experiment and the optical constants under consideration one may neglect the polarization dependence of the reflectivity. If one further assumes that $\epsilon_2^b(\omega) \ll \epsilon_2^s(\omega)$ and that $\epsilon_2^s(\omega)$ of the oxidized surface is small, one obtains

$$\alpha \sim \frac{\Delta R}{R} \sim \frac{8\pi}{\lambda} \frac{\sqrt{\epsilon_1^b}}{\epsilon_1^b - 1} d\epsilon_2^s(\omega) , \qquad (5.1)$$

with λ the wavelength of the light. The quantity $d\epsilon_2^s(\omega)$ can now be calculated from Fig. 4 of the paper of Chiarotti *et al.*[8] The result is plotted as a dotted line in Fig. 7. Obviously the peak S_0 in the ELS spectra and the reflectivity change in the multiple internal reflection experiment correspond to the same transitions. It has already been suggested by Chiarotti *et al.*[8] that these are transitions between occupied and empty parts of the dangling bond surface band. This interpretation is confirmed by a recent calculation of Betteridge and Heine[28] and also by the surface band-structure calculations of Pandey and Phillips,[6] which show that on the unreconstructed surface the Fermi level is approximately in the middle of the band. On the reconstructed 2×1 cleaved surface the dangling bond splits into two subbands giving rise to a optical absorption. This absorption is smaller on the annealed surface with 7×7 superlattice and exhibits no remarkable structure.[13]

Despite the general agreement between ELS and the optical result some quantitative differences remain (Fig. 7) which cannot be explained at the moment. A possible reason is that assumption (3.9b) is not very well fulfilled in the energy range around 0.5 eV. Quantitative agreement within the limit of accuracy of both methods is obtained with ellipsometry (Fig. 7). Again in ellipsometry the difference between ϵ_2^s of the clean and the oxydized surface (ϵ_2^* in Fig. 7) is measured,[9] while our method basically allows an absolute determination of optical properties. For energies higher than 3 eV, ϵ_2^b cannot be neglected any more (Fig. 2). In order to make the results comparable to ellipsometry we have sketched $d(\epsilon_2^s - \epsilon_2^b)$ by a broken line in Fig. 7. The comparatively large differences between ellipsometry and ELS for energies larger than 2.7 eV probably arise from the fact that ϵ_2^* of the oxydized surface is no longer equivalent to ϵ_2^b of the bulk in this energy range.[29] It seems useful to add some comments on the interpretation of ELS spectra that have been measured as first or second derivatives of the loss spectra. Recording of derivative spectra is necessary when analyzers of low resolution in energy and, even more importantly, in angle are used. Such second derivative spectra of surface states, e.g., have been reported by Rowe and Ibach[12] and Ludeke and Esaki.[23] It appears from these spectra that on the cleaved

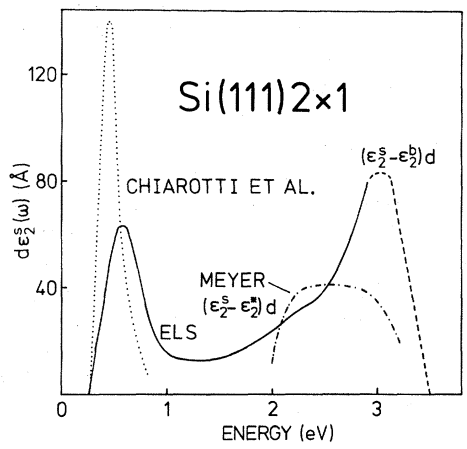

FIG. 7. Optical constant of the surface-state layer $d\epsilon_2^s(\omega)$ for silicon. The dotted line corresponds to the multiple-internal-reflection spectrum of Ref. 8. The dashed-dotted line is the result of ellipsometry (Ref. 9). In both optical methods the difference between bulk and surface $\epsilon_2(\omega)$ is measured. For energies up to 3 eV $\epsilon_2^b(\omega)$ may be neglected, as we did in our derivation. For higher energies the difference $\epsilon_2^s - \epsilon_2^b$ becomes small (see Fig. 2). This effect is indicated by the dashed line.

silicon surface a surface-state transition occurs at 2.2 eV. Comparison with Fig. 7 indicates that this transition is in fact only a tiny little hump on a continuous band of surface-state transitions. We therefore no longer regard the difference in the ELS derivative spectra between the cleaved and the annealed surface above 1 eV as very significant. For both surfaces a continuous band exists in the energy range between 1.5 and 3 eV. This explains why the two surfaces basically behave similarly in ellipsometry.

We have assumed that the absorption in Fig. 7 is mainly caused by transition between the two subbands of the dangling-bond surface band although bulk-state–to–surface-state transitions and *vice versa* may also contribute. The number of electrons contributing to the absorption should therefore be of the order of one electron per surface atom. In order to check the consistency of our data with this assumption we consider the f-sum rule

$$\int_0^\infty \epsilon_2(\omega')\omega' d\omega' = \frac{2\pi e^2}{m} N \,. \qquad (5.2)$$

N is the number of electrons per cm^3. The effective number of electrons per surface atom which contribute to an absorption at an energy $\hbar\omega$ is then

$$N_{\text{eff}} = \frac{1}{8\pi^2 a_B^3(R)^2 n_0} \int_0^{\hbar\omega} \hbar\omega' d\epsilon_2^s(\hbar\omega') d\hbar\omega' \,, \qquad (5.3)$$

with a_B the Bohr radius and n_0 the number of surface atoms per unit area. The effective number of electrons per surface atom calculated from the ELS data in Fig. 7 is plotted in Fig. 8. The total number of electrons involved in the surface absorption is indeed of the order of 1. This seems to give additional confidence in both the basic ingredients of the physical interpretation as well as in the procedure of a quantitative analysis of ELS data. It appears further from Fig. 8 that the optical absorption is indeed mainly due to transitions between surface states, although some cross transition surfaces to bulk and *vice versa* are also indicated by the rise in n_{eff} above 1. The total number of surface electrons contributing to the peak around 0.5 eV is only ~0.1 per surface atom. This may seem surprising at first glance. However, the total width of the occupied part of the surface band is ~1.8±0.3 eV.[1,2] Surface absorption is observed up to ~3.4 eV. With a band gap of 0.25 eV the width of the empty surface state band is estimated to be ~1.4 eV. The peak at 0.5 eV covers therefore only a very small fraction of both bands, and the sharp peak must be caused by a saddle point in the combined density of states.

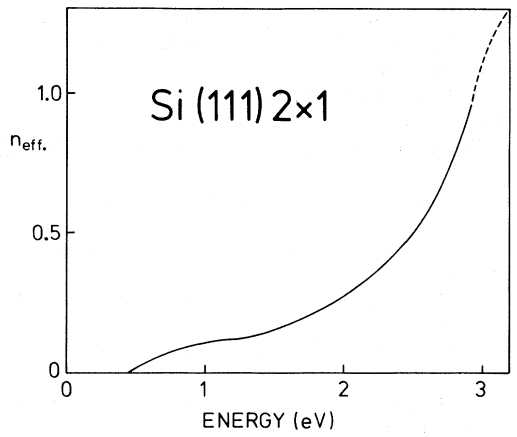

FIG. 8. Effective number of electrons per surface atom contributing to the optical absorption $d\epsilon_2^s(\omega)$ versus energy for silicon. Data for $d\epsilon_2^s(\omega)$ are taken from Fig. 7.

VI. SUMMARY

High-resolution energy-loss spectra obtained in specular reflection at various angles of incidence have been reported for cleaved surfaces of silicon and germanium. Features of these spectra can be attributed to surface and bulk interband transitions. Quantitative agreement between the inelastic cross sections for the bulk transitions and calculations according to a recently published extension of the dielectric scattering theory has been found. A surface optical absorption $d\epsilon_2^s(\omega)$ can be deduced from the surface contribution to the ELS spectra. For silicon the absolute value of $d\epsilon_2^s(\omega)$ as well as the energy dependence are in good agreement with results from previous optical experiments which were confined to more limited energy ranges. The effective number of electrons per surface atom contributing to the surface absorption $d\epsilon_2^s(\omega)$ up to ~3 eV has been calculated using the f-sum rule and was found to be roughly 1. This is consistent with the interpretation that the observed surface losses are due to transitions between the two subbands of the dangling-bond surface band.

We have seen in this paper that when electron-energy-loss data are combined with the theoretical model described above, one may obtain semiquantitative information about the nature of electronic surface states. These results should prove of value to theoretical studies currently under way.

ACKNOWLEDGMENT

The authors would like to thank G. Degen for assistance with the numerical calculations.

*Supported by the Air Force Office of Scientific Research, Office of Aerospace Research, U. S. A. F. under Grant No. AFOSR 71-2018.

[1]D. E. Eastman and W. D. Grobman, Phys. Rev. Lett. 28, 1378 (1972).
[2]L. F. Wagner and W. E. Spicer, Phys. Rev. Lett. 28, 1381 (1972).
[3]J. E. Rowe and H. Ibach, Phys. Rev. Lett. 32, 421 (1974).
[4]J. E. Rowe and J. C. Phillips, Phys. Rev. Lett. 32, 1351 (1974).
[5]J. A. Appelbaum and D. R. Hamann, Phys. Rev. Lett. 31, 106 (1973).
[6]K. C. Pandey and J. C. Phillips, Phys. Rev. Lett. 32, 1433 (1974).
[7]J. A. Appelbaum and D. R. Hamann, in Proceedings of the Twelfth International Conference on the Physics of Semiconductors, 1974 (unpublished).
[8]G. Chiarotti, S. Nannarone, R. Pastore, and P. Chiaradia, Phys. Rev. B 4, 3398 (1971).
[9]F. Meyer, Phys. Rev. B 9, 3622 (1974).
[10]F. Froitzheim and H. Ibach, Z. Phys. 269, 17 (1974).
[11]D. L. Mills, Surf. Sci. (to be published).
[12]J. E. Rowe and H. Ibach, Phys. Rev. Lett. 31, 102 (1973).
[13]J. E. Rowe, H. Froitzheim and H. Ibach, Surf. Sci. (to be published).
[14]R. Herzog, Z. Phys. 89, 447 (1934).
[15]D. Roy and J. D. Carette, Appl. Phys. Lett. 16, 413 (1970).
[16]H. Ibach, in Proceedings of the Twelfth International Conference on the Physics of Semiconductors, 1974 (unpublished).
[17]For a review see H. Raether, Springer Tracts Mod. Phys. 38, 85 (1965); J. Daniels, C. V. Festenberg, H. Raether, and K. Zeppenfeld, Springer Tracts Mod. Phys. 54, 77 (1970).
[18]A. A. Lucas and M. Sunjic Phys. Rev. Lett. 26, 229 (1971).
[19]A. A. Lucas and M. Sunjic, Prog. Surf. Science 2, 75 (1972).
[20]E. Evans and D. L. Mills, Phys. Rev. B 5, 4126 (1972).
[21]E. Evans and D. L. Mills, Phys. Rev. B 7, 853 (1973).
[22]L. van Hove, Phys. Rev. 95, 249 (1954).
[23]R. Ludeke and L. Esaki, IBM Research Report No. RC 4861 (unpublished).
[24]C. J. Powell, Phys. Rev. 175, 972 (1968).
[25]D. L. Mills and A. A. Maradudin (unpublished).
[26]R. C. Eden, Ph.D. thesis, Stanford University, available as dissertation No. 67-17, 415, University Microfilms, Inc., Ann Arbor, Michigan 48106 (unpublished).
[27]J. D. E. McIntyre and D. E. Aspnes, Surf. Science 24, 417 (1971).
[28]G. P. Betteridge and V. Heine, Surf. Sci. 43, 417 (1974).
[29]H. Ibach and J. E. Rowe, Phys. Rev. B 9, 1951 (1974).